agriculture

MDPI

Article

Potential Impact of Future Climates on Rice Production in Ecuador Determined Using Kobayashi's 'Very Simple Model'

Diego Portalanza [1,*], Finbarr G. Horgan [2,3,4], Valeria Pohlmann [5], Santiago Vianna Cuadra [6], Malena Torres-Ulloa [7], Eduardo Alava [7], Simone Ferraz [1] and Angelica Durigon [1]

1 Climate Research Group, Department of Physics, Federal University of Santa Maria, Av. Roraima, 1000, Santa Maria 97105-900, RS, Brazil
2 EcoLaVerna Integral Restoration Ecology, Bridestown, Kildinan, T56 P499 County Cork, Ireland
3 Facultad de Ciencias Agrarias y Forestales, Universidad Católica del Maule, Escuela de Agronomía, Casilla 7-D, Curicó 334900, Chile
4 Centre for Pesticide Suicide Prevention, Queen's Medical Research Institute, The University of Edinburgh, 47 Little France Crescent, Edinburgh EH16 4TJ, UK
5 Faculty of Agronomy, Department of Plant Science, Federal University of Pelotas, Pelotas 96010-610, RS, Brazil
6 Brazilian Agricultural Research Corporation (EMBRAPA), Brasília 70770-901, DF, Brazil
7 Escuela Superior Politécnica del Litoral, Facultad de Ciencias de la Vida, Guayaquil 090902, Ecuador
* Correspondence: diegoportalanza@gmail.com; Tel.: +593-994-043926 or +593-967-125056

Abstract: Rice (*Oryza sativa* L.) is the main staple food of more than 50% of the world's population. However, global production may need to increase by more than 70% before 2050 to meet global food requirements despite increasing challenges due to environmental degradation, a changing climate, and extreme weather events. Rice production in Ecuador, mainly concentrated in lowland tropical plains, declined in recent years. In this paper, we aim to calibrate and validate Kobayashi's 'Very Simple Model' (VSM) and, using downscaled corrected climate data, to quantify the potential impact of climate change on rice yields for Ecuador's two main rice-growing provinces. The negative impact is expected to be highest (up to −67%; 2946 tons) under the Representative Concentration Pathway (RCP) 8.5, with a lower impact under RCP 2.6 (−36%; 1650 tons) yield reduction in the Guayas province. A positive impact on yield is predicted for Los Ríos Province (up to 9%; 161 tons) under RCP 8.5. These different impacts indicate the utility of fine-scale analyses using simple models to make predictions that are relevant to regional production scenarios. Our prediction of possible changes in rice productivity can help policymakers define a variety of requirements to meet the demands of a changing climate.

Keywords: agricultural modeling; rice; climate change; RCPs; yield gaps

Citation: Portalanza, D.; Horgan, F.G.; Pohlmann, V.; Vianna Cuadra, S.; Torres-Ulloa, M.; Alava, E.; Ferraz, S.; Durigon, A. Potential Impact of Future Climates on Rice Production in Ecuador Determined Using Kobayashi's 'Very Simple Model'. *Agriculture* **2022**, *12*, 1828. https://doi.org/10.3390/agriculture12111828

Academic Editors: Arnd Jürgen Kuhn, Giuseppe Fenu, Hazem M. Kalaji and Branka Salopek-Sondi

Received: 8 September 2022
Accepted: 21 October 2022
Published: 1 November 2022

1. Introduction

Rice (*Oryza sativa* L.) is the main staple food for more than 50% of the world's population [1,2]. Estimates vary with respect to the requirements for increased rice production to meet the world's growing human population. In areas of intensive rice production in Asia, estimates of up to 2% annual increases in production have been proposed to meet regional demands [3]; globally, production may need to increase by over 70% before 2050 to meet the food requirements associated with global population and economic expansion [4]. Meeting these global requirements for rice production is, however, increasingly challenged by environmental degradation [5], a changing climate, and extreme weather events [6].

Rice production in Ecuador is concentrated mainly in the lowland tropical plains, where there are marked wet (December–May) and dry (June–November) seasons. This region produces up to 1.5 million tons of rice grain annually. Much of this production occurs in the Provinces of Guayas (235 K ha—54%) and Los Ríos (115 K ha—33%). Rice is also produced in Manabí Province (12 K ha; 7.15%), Loja (5–6 K ha, 0.47%), El Oro (2–3 K ha;

0.37%), Esmeraldas (<100 ha; 0.54%), and other provinces 3.37% [7–9]. In Ecuador, the area dedicated to rice production declined in recent years [10] from an average of about 400,000 ha before 2015 to 301,853 ha in 2018 [11,12].

This downward trend is associated with the production of alternative crops, including upland crops such as maize (*Zea Mays* L.) and soybean (*Glycine max* (L) Mirr.). The abandonment of rice due to production constraints (including pests) and production costs alarmed the government because rice production plays a vital role in Ecuador's food security and is a prevalent activity that secures rural livelihoods in many parts of the country [13].

Ensuring that rice production is maintained and productivity increases over the coming decades will be important to ensure the long-term sustainability of rural communities and possible rice self-sufficiency for Ecuador in the face of projected environmental changes, including projected increases in atmospheric CO_2 concentrations. The effects of elevated CO_2, which results mainly from the burning of fossil fuels, on global rice productivity have been difficult to predict because different aspects of climate change affect rice crops differently and predominant farming practices may largely determine production responses to future climates [14]. However, estimating regional production responses to predicted changes in atmospheric CO_2 and climate, which is likely to be more accurate, may be useful in directing government policies to secure national food production. Predicting the future of rice production requires models that combine details of crop growth dynamics, fluctuating environmental conditions—including climatic conditions—and prevailing production practices [4,15].

Several studies indicate that climate change has already had induced negative consequences on agriculture and could reduce crop productivity in the future [16–18]. While increasing atmospheric CO_2 could benefit rice plants via increased photosynthesis (CO_2 fertilization), a projected increase of 0.02 °C annually in mean global temperatures during the coming two to three decades [19,20] could significantly affect rice production via temperature stresses (particularly on flower sterility) and evapotranspiration [21]. Such temperature-associated effects on rice productivity are likely to be most severe in lowland tropical regions and, therefore, potentially threaten Ecuador's future rice production capacity. Suitable adaptation strategies can help mitigate such effects of climate change; therefore, many integrated models have been developed to assess the impact of climate change on agriculture [15].

Recently, advanced state-of-the-art climate projection datasets derived from global climate models (GCM) have become widely available [19,22,23]. These datasets are associated with four Representative Concentration Pathways (RCPs: 2.6 4.5, 6.0, and 8.5) [24] identified by the Intergovernmental Panel on Climate Change (IPPC) as encompassing future likely scenarios related to the burning of fossil fuels and consequent atmospheric CO_2 concentrations. These freely available datasets are customarily only distributed at coarse resolution, which is adequate for casual weather and climate studies. However, to support agricultural decision making, GCM datasets must be interpreted to the final users' domain using various post-processing methods, including bias correction, adjustment, and downscaling [25,26].

Crop growth simulation models are valuable tools for inferring from the results of field experiments and projecting the differential effects of various crop management practices over distinct climatic periods and environments. Such simulation models can characterize the complex relationships between crop genotype, crop management practices, and climate [27]. Furthermore, when sufficiently calibrated and validated, these crop models represent a systems approach for evaluating potential crop management responses to climate and the potential behavioral changes expected from stakeholders [28].

Despite their utility, crop models are frequently so complicated that they become difficult to comprehend. Furthermore, some of the high-resolution input data may not be accessible or is unavailable in some countries. To deal with these shortcomings, Kobayashi (1994) developed a 'Very Simple Model' (VSM) to determine crop growth based on three principal assumptions: (1) that the leaf area index (LAI) develops in a triangular manner,

(2) that biomass is grown equitably with solar radiation interception, and (3) that crop yield can be simply represented by total biomass at harvest multiplied by the harvest index. A comprehensive description of the model is given by Kobayashi (1994) and Pirmoradian and Sepaskhah (2006). The model assumes that rice is protected against pests and diseases and does not consider productivity decreases due to these outer factors [29,30].

Since Ecuador lacks studies using rice crop modeling to establish climate impacts [31], in this paper, we aim to perform the following: (a) validate the VSM; and (b) using downscaled corrected data for RCPs, quantify potential impacts of the changing climate on rice yields for Ecuador's two main rice-growing regions (Guayas and Los Ríos). By applying the VSM for rice production in Ecuador, we develop a useful baseline for future crop-modeling studies.

2. Materials and Methods

2.1. Study Area

The Rice Land Use and Land Cover (LULC) area, which comprises two main productive Ecuadorian provinces, Guayas (GP) (54%) and Los Ríos (LRP) (33%), was selected as the study area (Figure 1).

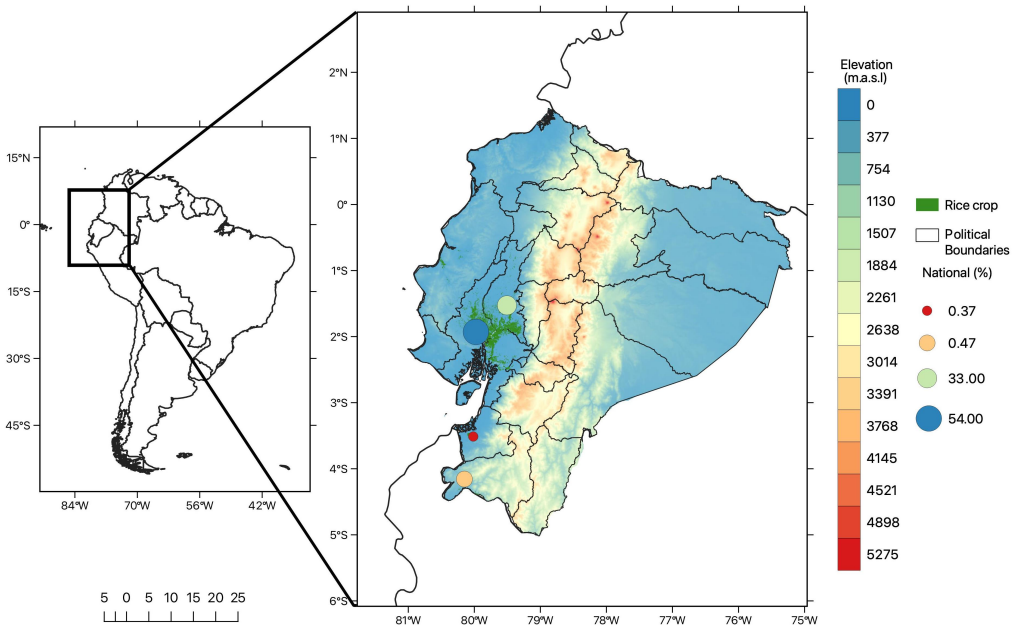

Figure 1. Study region. Spatial distribution of rice crop [32]. The colored dots represent the national percentage (hectares) of the main producing provinces.

2.2. Data and Methods

2.2.1. Description of the Very Simple Model (VSM)

Kobayashi (1994) presented a very simple model for determining crop growth. The model can be expressed in one line; hence, VSM outputs are easy to interpret. The VSM crop simulation model [29] was used to simulate rice growth and yields to analyze future impacts of a changing climate. The VSM was run based on three assumptions: Firstly, that LAI fluctuates in a triangular manner as follows:

$$\begin{aligned} L &= 0 \; for \; 0 < t \leq T_0 \\ L &= \alpha(t - T_0) = L_f(t - T_0)/(T_f - T_0), for \; T_0 < t \leq T_f \\ L &= L_f - \beta(t - T_f) = L_f[1 - (t - T_f)/(T_h - T_f)], for \; T_f < t \leq T_h \end{aligned} \quad (1)$$

where L is the LAI; t is the period after emergence (in days (d)); α is the daily increase in LAI; T_0 is the period from emergence to linear increase in LAI (in d); L_f is the maximum LAI in

the flowering season T_f; b is the daily decrease in LAI; T_h is the period from emergence to harvest (in d).

Second, the biomass is stored uniformly relative to the captured solar radiation as follows:

$$dW/dt = \epsilon S[1 - \exp(-kL)] \quad (2)$$

where dW/dt is the daily accumulation of biomass (g m^{-2} d^{-1}); e is the light use efficiency (g MJ^{-1}); S is the shortwave solar radiation (MJ m^{-2} d^{-1}); k is the light extinction coefficient.

The yield is denoted as the total biomass at harvest multiplied by the harvest index:

$$Y = W_h I_H \quad (3)$$

where Y is the grain yield (g m^{-2}), W_h is the total dry weight at harvest (g m^{-2}), and I_H is the harvest index as a grain fraction of the total biomass [30].

The total dry matter is calculated by integrating the daily biomass accumulation. Considering the above assumptions, the integral can be simplified as follows [29]:

$$\begin{aligned} W_h &= \int_0^{T_h} \epsilon s[1 - \exp(-kL)]dt \\ &\approx v\epsilon_v \int_0^{T_f} [1 - \exp(-kL)]dt + r\epsilon_r \int_{t_f}^{T_h} [1 - \exp(-kL)]dt \\ &= v\epsilon_v\{1 - [1 - \exp(-k\alpha T_v)]/(k\alpha T_v)\} + r\epsilon_r\{1 - [1 - \exp(-k\beta T_r)]/(k\beta T_r)\} \\ &\approx 0.85v\epsilon_v T_v[1 - \exp(-0.55k\alpha T_v)] + 0.85r\epsilon_r T_r[1 - \exp(-0.55k\beta T_r)] \\ &\approx 0.85[1 - \exp(-0.55kL_f)](vT_v\epsilon_v + rT_r\epsilon_r) \end{aligned} \quad (4)$$

where period T_v (days), which denotes the period from the beginning of the linear increase in LAI to flowering, and period T_r (days), which denotes the period from flowering to harvest, are given by $T_v = T_f - T_0$ and $T_r = T_h - T_f$, respectively; v and r are the daily mean shortwave radiation before and after flowering (MJ m^{-2} d^{-1}) for T_v and T_r, respectively; ϵ_v and ϵ_r are the light-use efficiency (g MJ^{-1}) for T_v and T_r, respectively; k is the light extinction coefficient.

Simulations were carried out for a rain-fed rice season considering 16 December as a fixed sowing date for both region's yearly for reference period 1975–2005 and all RCPs (2070–2100).

2.2.2. Input Data Processing

Ecuadorian rice paddy areas were extracted from the National LULC database provided by the Ecuadorian Ministry of Agriculture and Livestock [32]. With this map, we filtered rice provincial areas from Guayas and Los Ríos. First, we extracted rice shapefile masks and rasterized them in NetCDF format using the Geospatial Data Abstraction Software Library (GDAL) [33].

Data from the Hadley Centre Global Environmental Model 2-Earth System (HadGEM2-ES) model, one of the most used models for the IPCC Fifth Assessment Report (AR5), are used as boundary conditions to drive the Regional Climate Model (RCM) dynamic downscaling [34,35].

Daily precipitation (mm d^{-1}), incident visible solar energy flux (MJ m^{-2} d^{-1}), u component (west) of wind, v component (south) of wind, maximum and minimum air temperatures (°C), surface pressure (hPa), and specific humidity (kg kg^{-1}) data for 1975–2005 (reference period) and 2070–2100 (future period) were obtained from the Regional Climate Modeling System's (RegCM4) [36,37] downscaled datasets for Ecuador. Regional simulations with RegCM4 were generated in a domain centered over Ecuador, Northern South America, with a latitude of projection origin at −1.5 and a longitude of projection origin at −78. The extracted data were then regridded to the RCM dataset using the Climate

Data Operators (CDO) software [38] remapbil command to ensure that the resolution was equivalent. The daily climate data for both regions were then extracted using the National Center for Atmospheric Research Command Language (NCL) [39].

Finally, we constructed a provincial database for the same climatic variables for the daily climate reference period (RP) (1975–2005), and future period (FP) (2070–2100) for 3 possible climate change scenarios (RCPs: 2.6, 4.5, and 8.5) [40–42] representing greenhouse gas (GHG) emissions that can lead to radiative forcing levels up to 2.6, 4.5, and 8.5 (W m^{-2}) in that order [21].

Model initial configuration and VSM parametrization are described in Supplementary Materials (Table S1) [43–45]. Annual model output files (NetCDF) were collected using CDO to facilitate data exploration and visualization.

Wind speed (ws) was calculated as follows:

$$ws = \sqrt{(u^2 + v^2\ )} \tag{5}$$

where u is the westerly component of the wind, and v is the southerly component of the wind.

The relative humidity (RH) was calculated as follows:

$$RH = \frac{Q * P}{\frac{0.622+0.378Q}{e_s}} * 100 \tag{6}$$

where RH is the relative humidity, Q is the specific humidity, P is the surface pressure, and e_s is the saturation vapor pressure. The saturation vapor's pressure was estimated using the Clausius–Clapeyron relation as follows:

$$e_s = e_s(T_0)^{(\frac{L}{R_W}(\frac{1}{T_0}-\frac{1}{T}))} \tag{7}$$

where $e_s(T_0)$ = 6.11 hPa is the saturation vapor pressure at the reference temperature T_0 = 273.15 K, L is the latent heat of evaporation for water, and R_w is the specific gas constant [46].

Bias correction was performed using the quantile mapping approach [47–49] with the ERA5 dataset [50–52]. To this end, RCM outputs were re-gridded to the ERA5 grid. The performance of bias-corrected data was tested against down-scaled data.

2.2.3. Climate Change Impact Assessment

VSM was set up and run covering Guayas and Los Ríos Provinces. The performance of the model was evaluated by comparing the yield simulated by historical weather data (1975–2005) with the RCM's yield outputs. The reference period (1975–2005) was separated into two databases for model calibration (1983–1993) and validation (1994–2005). We excluded the 1975–1982 period since observed data were not available. Then, we used graphical representations and statistical approaches to evaluate the performance of the model in predicting biomass and yield.

The following goodness-of-fit measures (GOF) were used: coefficient of determination (R^2), mean error (ME), mean absolute error (MAE), root mean square error (RMSE), normalized mean square error (RMSEn), index of agreement (d), and modified index of agreement (d) [53,54]. GOFs were calculated using the hydroGOF package [55] for Rstudio [56] and plotted with the ggplot2 package [57,58]. The equations for the GOF measures were as follows:

$$MAE = \frac{1}{n}\sum_{i=1}^{n}(P_i - Q) \quad (8)$$

$$RMSE = (\sum_{i=1}^{n}(P_i - Q_i)^{\frac{2}{n}})^{\frac{1}{2}} \quad (9)$$

$$RMSE_n = \frac{\sum_{i=1}^{n}(P_i - Q_i)^{\frac{2}{n}})^{\frac{1}{2}}}{M} * 100 \quad (10)$$

$$d = 1 - [\frac{\sum_{i=1}^{n}(P_i - Q_i)^2}{\sum_{i=1}^{n}(|P_i| - |Q_i|)^2}] \quad (11)$$

where P_i and Q_i refer to the predicted and calculated data, respectively, n is the number of observations, M is the mean of the observed occurrence, and $|P_i| = P_i - \mathrm{M}$ and $|Q_i| = Q_i - \mathrm{M}$.

After establishing the suitability of the VSM, future climate change impacts on rice yield were examined by comparing simulated rice yields for the 30-year base period (1975–2005) using RP RCM data for Guayas and Los Ríos Provinces with simulated rice yield by using the RCM dataset for the three different RCP scenarios for the future period (2070–2100). With this method, a total of 240 simulations were performed (30 years × 4 periods × 2 provinces) by considering increased atmospheric CO_2 for RCP 2.6, 4.5, and 8.5. Results were expressed as percentages.

3. Results

3.1. Projected Mean Change in Climatic Variables Based on RegCM4

Precipitation showed a marked pattern for the lowlands with less precipitation overall (Figure 2). The total accumulated precipitation in Guayas is approximately 540 and 750 mm, while in Los Ríos, it could be up to 2000 mm. The months from January to April are expected to show a high accumulated precipitation of around 690 mm in Los Ríos and 400 mm in Guayas. The monthly precipitation cycle for the lowlands showed that December, January, and February are the months with higher values since they represent the rainy season.

Results showed that greater mean temperatures are observed in Guayas Province than in Los Ríos. The aggregated mean temperature for Guayas is 26.01 °C, with January and December being the months with lower mean temperatures of 25.27 and 25.18 °C, respectively. For Los Ríos, the average mean temperature was 21.24 °C (Figure 2C). A more detailed provinces comparison is shown in Supplementary material Table S2.

Mean seasonal changes under RCP2.6, 4.5 and 8.5 are indicated for rainfall in Figure 2B and temperature in Figure 2D. The outcome of the model shows that precipitation is expected to increase by 3 to 20%, 10–54%, and 20–40% in all zones by 2100 under RCP 2.6, RCP 4.5, and RCP 8.5 scenarios, respectively. For precipitation, the lowlands showed a positive mean monthly change of 20% (RCP 2.6), while for the rest of the country values of 50% in the same RCP are shown. Precipitation for RCP 4.5 showed equal RCP 2.6 shifts for the central and western lowlands at −20%. Guayas and Los Ríos showed a mean daily positive change of 1.75 (mm).

Mean temperatures are also predicted to increase by between 1 and 5 °C in all zones under different climate scenarios. For RPC 2.6, the temperature will have a mean change of 1.61 and 1.68 °C for the lowlands and highlands, respectively. The mean air temperature values showed a strong trend for RCP 4.5 and RCP 8.5 across regions, with the western part of the lowlands (part of Los Ríos) and the southern part indicated as increasing by 2.63 and 2.38 °C, respectively.

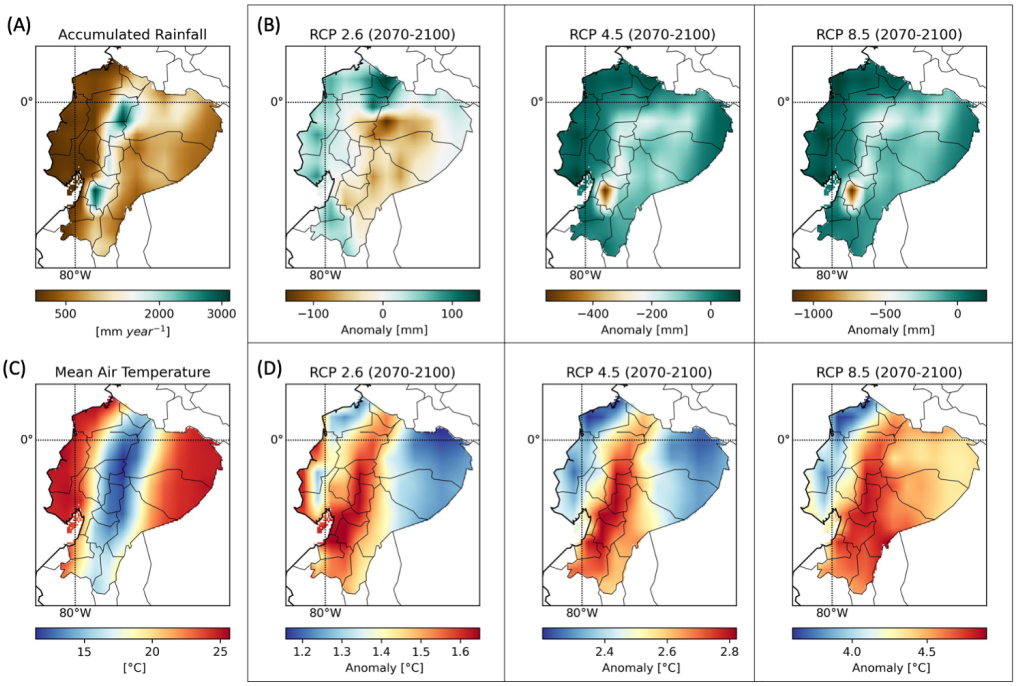

Figure 2. Annual precipitation (**A**) and mean air temperature (**C**) climatology. Seasonal mean change in (**B**) rainfall (%) and (**D**) mean air temperature with respect to the base period (1975–2005) predicted based on RegCM4 daily weather for 2070–2100 under RCP 2.6, 4.5, and 8.5 scenarios.

3.2. Model Suitability Confirmation

Figure 3 shows the correlations between the simulated and observed yields for the calibration dataset: the correlation coefficients are 0.98 for Guayas (Figure 3A) and 0.81 for Los Ríos (Figure 3B). A high level of precision was obtained in simulations with an RMSE of 793 kg ha^{-1} and 298 kg ha^{-1} and an nRMSE of 55 kg ha^{-1} and 123 kg ha^{-1} (Table 1), for Guayas and Los Ríos, respectively, representing good agreements between observed and simulated tendencies.

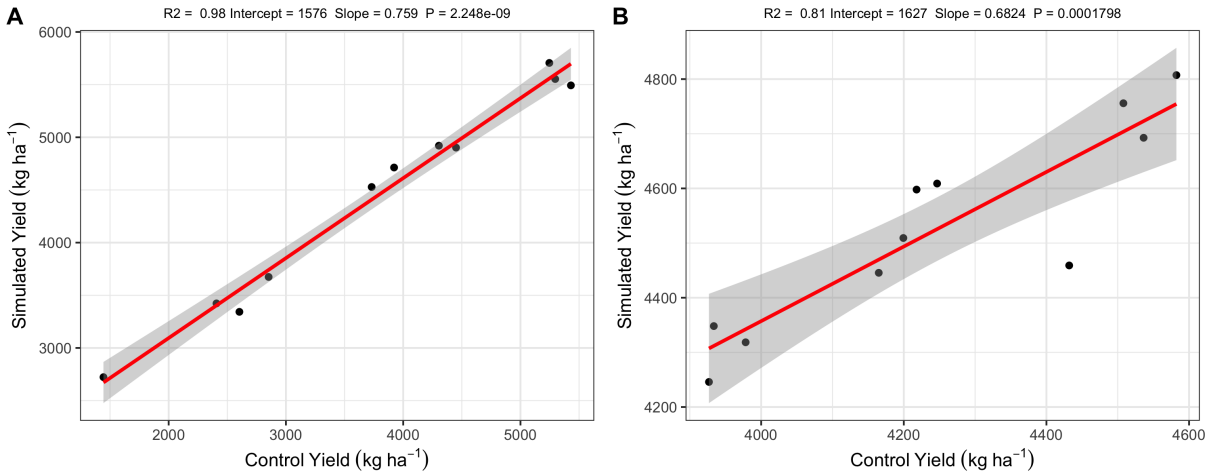

Figure 3. Correlations between yearly simulated and observed (control) total yields corresponding to the 1983–1993 calibration data set for Guayas (**A**) and Los Ríos (**B**) Provinces. The red lines represent fitted linear regressions lines, and the gray-shaded areas represent 95% confidence intervals.

Furthermore, indices of agreement (d) were 0.90 (Guayas) and 0.67 (Los Ríos). The percentage of biased data (PBIAS) was relatively low with 17 % and 6% for Guayas and Los Ríos, respectively. The values were close to those observed during data validation

(Figure 4). Observed and estimated data were highly correlated ($R^2 > 0.85$), except for the calibration data for Los Ríos (Table 1).

Table 1. Evaluation results for VSM yield simulations over the entire growing season for calibration and validation datasets for Guayas and Los Ríos Provinces.

Dataset	Site	Control (SD)	Sim (SD)	α	β	R	RMSE	RMSEn	MAE	*d*	PBIAS
Calibration	**Guayas**	3789.83 (1323)	4452.57 (1012)	1576.00	0.76	0.98	739.36	55.90	66.62	0.90	17.50
	Los Ríos	4247.81 (241)	4526.25 (183)	1627.39	0.68	0.81	298.01	123.6	278.44	0.67	6.6
Validation	**Guayas**	3619.60 (1418)	4181.15 (1166)	1231.00	0.82	0.98	632.69	44.60	561.55	0.94	15.50
	Los Ríos	4045.75 (291)	4295.21 (237)	1253.00	0.75	0.85	273.04	93.70	249.46	0.77	6.20

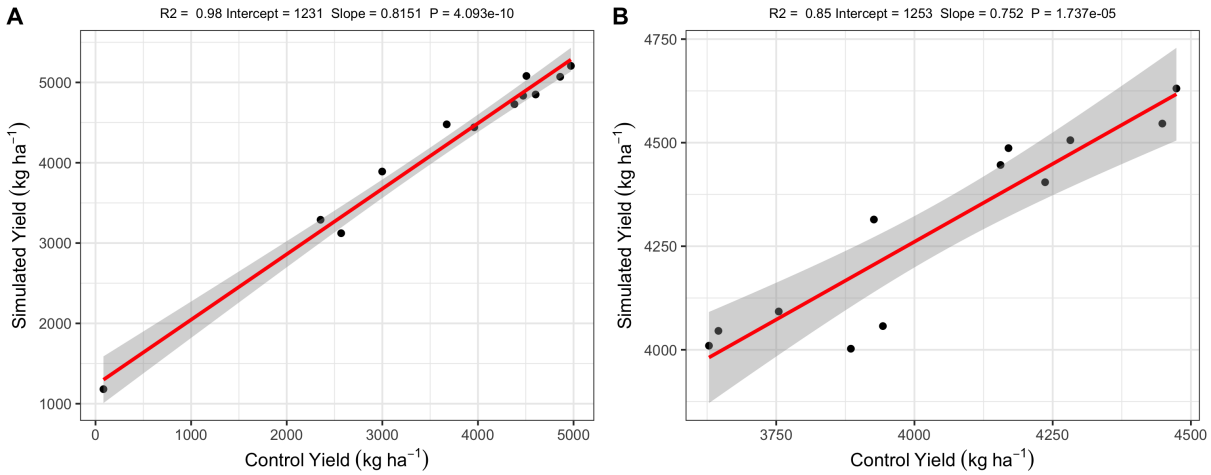

Figure 4. Correlations between yearly simulated and observed (control) total yields corresponding to the 1994–2005 validation data set for Guayas (**A**) and Los Ríos (**B**) Provinces. The red lines represent fitted linear regression lines, and the gray-shaded areas represent 95% confidence intervals.

The data fit was better for Guayas than Los Ríos. The RMSE found in this study is superior to those found for the productivity of hybrid rice adjusted to ORYZA version 3, with an RMSE of 175 kg ha^{-1} [2]. However, the RMSE values between simulated and observed data were lower than the standard deviation of the observed data, which according to Gaydon et al (2017) [59] demonstrates that the model simulates the observed behavior within the limits of experimental error.

3.3. Model Results

Rice yield was simulated and averaged for RP (1975–2005) (Figure 5A) and FP (2070–2100) for RCP 2.6, 4.5, and 8.5 (Figure 5B–D) for the Provinces of Guayas and Los Ríos for influence analysis. The simulated yields for Guayas indicate that the predicted future climatic variables (temperature, precipitation, and solar radiation) will cause a decrease in yields under all three RCPs.

The spatial yield-change differed between Guayas and Los Ríos. It is clear from Figure 5A that all RegCM4-VSM simulations for Guayas depict a negative impact on yields under all climate scenarios (Table 2). This negative impact is expected to be highest (i.e., up to −67%; 2946 tons) under RCP 8.5, with a lower impact under RCP 2.6 (i.e., −36%; 1650 tons) yield reduction. A positive impact on yield is predicted for the Los Ríos Province (i.e., up to 9%; 161 tons) under RCP 8.5 (Figure 5D, blue lines).

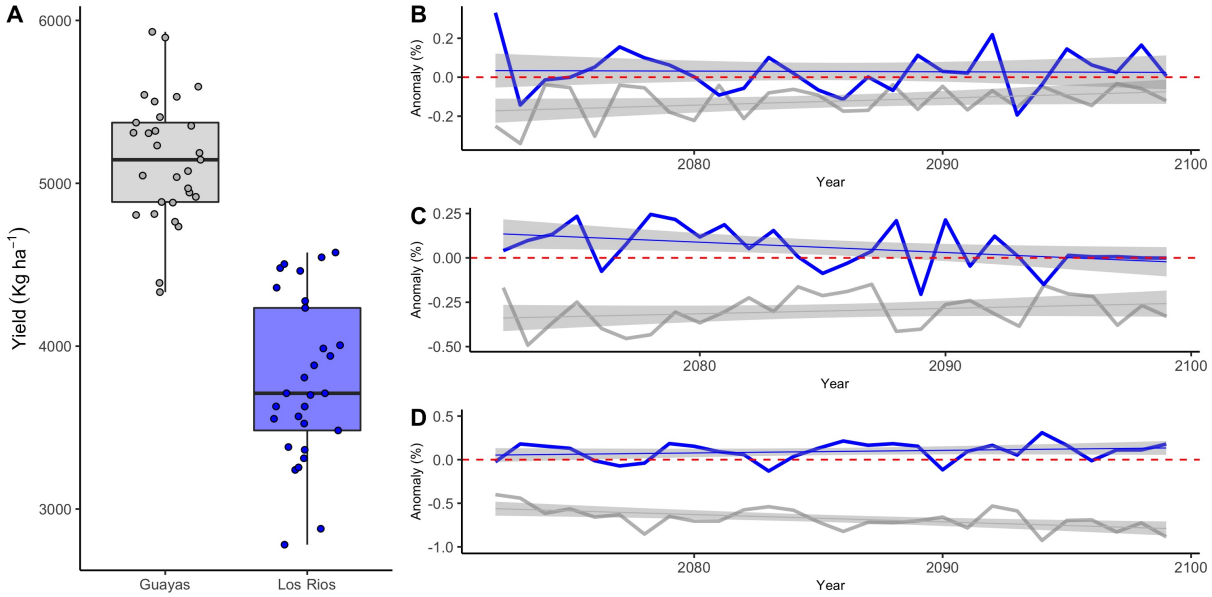

Figure 5. Percent change in rice yields estimated from the RegCM4 RP VSM output (**A**) for the Provinces of Guayas (gray) and Los Ríos (blue) with corresponding changes over the time period under RCP 2.6 (**B**), RCP 4.5 (**C**), and RCP 8.5 (**D**) as related to the yields of the base period (1975–2005). The lines represent changes in yield over time. Grey shaded areas in (**B**–**D**) represent 95% prediction confidence.

Table 2. Percentage yield, harvest day, and biomass change with respect to RP (1975–2005).

	Yield	Harvest Day	Biomass
Guayas *	−0.3658	−0.1902	−0.3014
RCP 2.6	−0.1236	−0.0765	−0.1168
RCP 4.5	−0.2982	−0.1477	−0.2494
RCP 8.5	−0.6756	−0.3463	−0.5380
Los Rios *	+0.0598	−0.0773	+0.0131
RCP 2.6	+0.0294	+0.0235	−0.0148
RCP 4.5	+0.0563	−0.0667	+0.0146
RCP 8.5	+0.0935	−0.1889	+0.0395

* Rows represent RCPs ensemble means.

Changes in total rice biomass had the same patterns as yield projections for Guayas and Los Ríos (Figure 6). On average, Guayas presents a mean RF biomass of 11,151 tons, whereas for Los Ríos it is 8715 tons (Figure 6A). Negative trends will occur for Guayas under all RCPs (Figure 5B–D). A mean negative 30% (3511 tons) and a maximum negative 53% for the RCP 8.5 (Table 2) are predicted. For Los Ríos, a biomass increase is expected, but to a lesser degree (about 0.013%; 53 tons). Based on temperature and solar radiation projections, these changes are predicted to be greater in Los Ríos.

For harvest days, that is, total cycle days (Figure 7), predicted average RCPs resulted in a 20% reduction in the crop cycle for Guayas (22 days) but an increase of 0.07% (13 days) is expected for Los Ríos. The projection of RCP 8.5 resulted in a 34% reduction for Guayas while an 18% reduction was observed for Los Ríos.

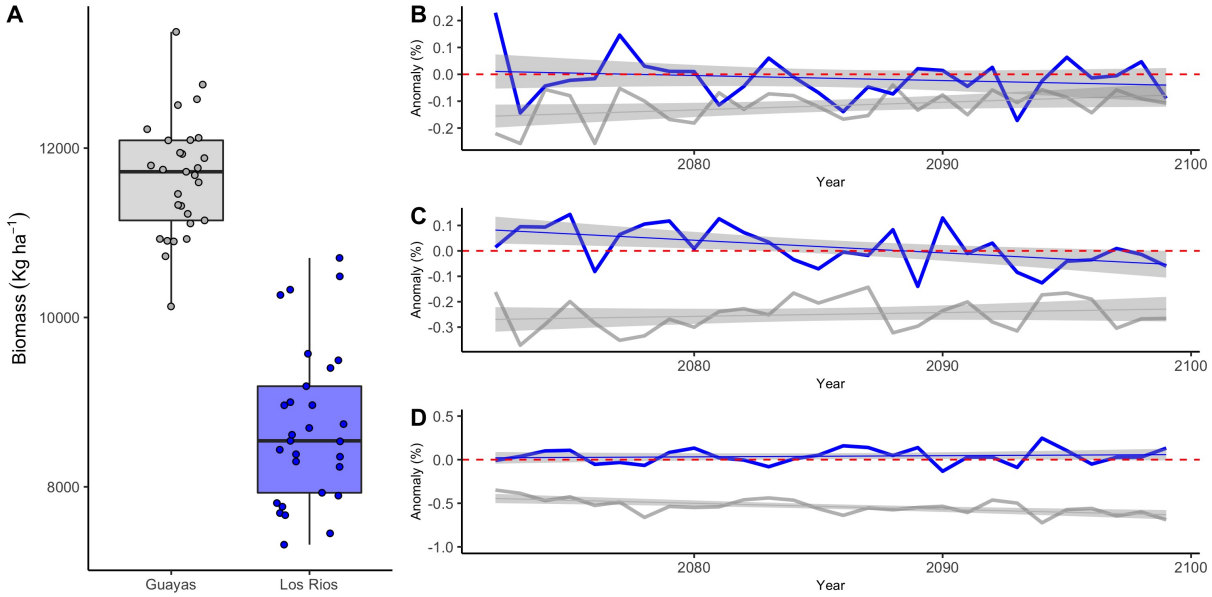

Figure 6. Percent change anomalies in rice total biomass projected from the RegCM4 RP VSM production (**A**) for the provinces of Guayas (gray) and Los Ríos (blue), with corresponding changes over the time period under RCP 2.6 (**B**), RCP 4.5 (**C**), and RCP 8.5 (**D**). The lines represent the annual changes in yield. Grey-shaded areas in (**B**–**D**) represent 95% prediction confidence.

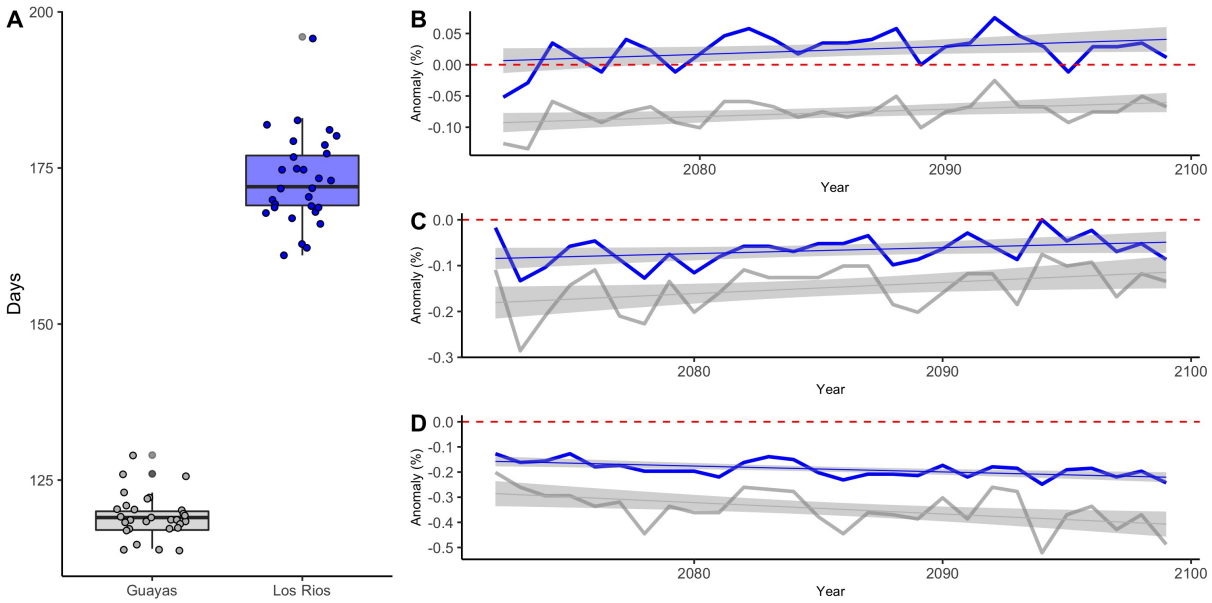

Figure 7. Percent change anomalies in rice harvest day projected from RegCM4 RP VSM output (**A**) for Guayas (gray), and Los Ríos (blue) Provinces with corresponding changes over the time period under RCP 2.6 (**B**), RCP 4.5 (**C**), and RCP 8.5 (**D**). The lines represent the annual changes in yield. Grey shaded areas in (**B**–**D**) represent 95% prediction confidence.

4. Discussion

To date, rising global temperatures have been accompanied by considerable changes in human and natural systems, including more frequent droughts, floods, and other extreme weather events; sea-level rise; and biodiversity loss [60]. These changes will bring extraordinary risks for vulnerable people and cultures, including populations located along coastlines or in low-lying coastal areas [41]. Many of the most affected people live in low-

and middle-income countries, such as Ecuador, some of which are already experiencing declining food security.

These hazards from climate change vary with the scale and degree of warming, geographic location, levels of development, and vulnerability and on the adoption and application of adaptation and mitigation measures by governments [61]. For coastal and highland regions, these trends could result in yield reductions of maize, rice, wheat, and potentially other cereal crops, affecting smallholder farmers with little or zero adaptation or mitigation measures [62].

Our estimates of yield reductions are higher than those from similar predictive studies for rice production regions in Asia. Using the same meteorological variables, Dinh et al (2020) [63] evaluated the spatial variations in rice yield losses in China using the CSM-CERES-Rice model of the Process-Based Decision Support System for Agrotechnology Transfer (DSSAT), using different combinations of the GCM, and predicted yield decreases of 22–22.7% in agroecological zones similar to Ecuador.

Furthermore, from the Coordinated Regional Climate Downscaling Experiment (CORDEX) [64], using three RCMs Chun et al (2016) [65] evaluated rice productivity using a multiscale crop model (GLAM-Rice and CERES-Rice) for Southeast Asia. These authors predicted that yield reductions under projected climate changes will be the greatest, nearly 45% in the 2080s under RCP 8.5, relative to their selected baseline period (1991–2000). Despite this, it is estimated that areas for rice will actually increase in the tropics under RCP 4.5 and RCP 8.5 scenarios [66]

Our results are similar to predictions by Su et al (2021) [66] based on field experiment data and the novel ORYZA version 3 [2,67]. These authors suggested that increased temperatures and/or changes in precipitation could reduce mean rice yields by 9.4% under RCP 4.5 and by 47.9% under RCP 8.5 for the 2080s scenario. In contrast, Arunrat et al (2018) [68] studied the predicted local-scale impact of climate change on rice yields to suggest that all rice yields under RCP 6.0 (2080–2090) will tend to increase by 0.7%, while under RCP 8.5, rice yields will decrease by 8.4%. Increasing rice yields under a changing climate are predicted to occur in response to carbon fertilization under higher future CO_2 levels [69].

Using a Soil and Water Assessment Tool (SWAT) with HadGEM2-ES model data, Mandal et al (2021) [70] assessed the impact of climate change on hydrological regimens and biomass yields of the Subarnarekha tropical river basin (north-east corner of Peninsular India). The authors found that the basin was likely to experience a loss of crop biomass (rice, wheat, and maize) of 2 to 3% due to climate change.

Based on temperature and solar radiation projections, our model suggests that these changes (delta anomalies) are expected to be greater in Los Ríos, and a higher atmospheric intensity of CO_2 (RCP 8.5) could increase photosynthesis, biomass accrual and production [71,72]. Therefore, the impact of climate change on rice crop yields could be positive in some agricultural provinces and adverse in others [73].

Our model projection under RCP 8.5 predicted a 34% reduction for Guayas and an 18% reduction for Los Ríos. The authors of Li et al (2017) [67] showed that the magnitude of the reduction in the length of the rice-growing season varies between single, early, and late rice genotypes when exposed to changes in temperatures and high-humidity periods. An increase in nighttime temperatures can accelerate the crop cycle due to greater thermal sum accumulation [74], but it can also affect spikelet ferility, resulting in higher levels of sterility and reduced grain filling or final grain quality [75].

Our results are also in agreement with those reported by Ding et al (2017) [76]; they used a length calculation method model and a daily water balance to detect spatial patterns, resulting in shortened trends in historical and future periods by up to 10 days in the 2080s under the RCP 8.5 scenario.

Based on the findings, changing planting dates and adapting to new rice cultivars can be beneficial for the adaptation of rice cultivation under climate change scenarios in Ecuadorian rice areas [77,78]. Resulting yield forecasts of crop models based on various

GCMs and RCPs can deliver more consistent climate change impact evaluations [79,80]. Therefore, future projections for economically important Ecuadorian crops should consider using several model databases.

Furthermore, to adapt to the effects of climate change on rice production, a dynamic cropping calendar, the development of irrigation schemes, and combined plant nutrient management could be established for agribusiness practices based on our preliminary results in the study area [70]. Our analysis is not only the first assessment of the impact of climate change on rice yields but it also highlights current deficiencies in rice production that risk Ecuadorian food security.

The amount and distribution of precipitation and temperature anomalies are imperative for crop production [23], and it is difficult to accurately predict the potential volumes and distribution of rainfall, and indexes based on temperature, monitoring, and observed assessments are necessary to detect these projections [22].

To facilitate agrometeorological management more, improved agro-meteorological stations need to be set up in Ecuador based on cropland covers. Therefore, close monitoring and evaluation for detecting the direction of future changes together with the development of flexible adaptation strategies are essential to deal with climate change [16]. The predicted effects of projected RCPs on rice production vary between studies according to region and crop production practices. Our study indicates largely distinct impacts of projected future climates on rice production in Guayas and Los Ríos. Under two of the RCPs, rice biomass accumulation and yields are predicted to decline in Guayas but increase in Los Ríos. Similarly, while crop durations are expected to decrease in Guayas, durations may increase in Los Ríos.

These different impacts indicate the utility of fine-scale analyses using simple models to make predictions that are relevant to regional production scenarios [25]. The distinct biomass and yield responses for the two regions are mainly derived from increasing temperatures and solar radiation in the warmer lowlands of Guayas, which reduce rice productivity by shortening the crop cycle. Crop duration is one of the main drivers of rice yields. However, changes in crop duration could also affect the impact of diseases and insect pests on rice [2]. For example, longer-duration varieties are exposed to field pests for longer and are, therefore, more vulnerable to insect attacks [81]. Therefore, a decline in pest incidences could be predicted in Guayas but they are predicted to increase in Los Ríos independently of the effects on herbivore voltinism (i.e., the number of generations per crop season [82]) associated with higher temperatures.

Our prediction of possible changes in rice productivity can help policymakers define a variety of requirements to meet the demands of future climates. However, the predicted effects of CO_2 on yields, as indicated in this study, should also encourage policymakers to find alternatives to the burning of fossil fuels for energy production.

5. Conclusions

The findings in this research show that projected RCPs on rain-fed rice production vary between sites based on regional conditions and crop production practices, resulting in largely distinct impacts of projected future climate on rice production in Guayas and Los Ríos.

Under several RCPs, rice biomass accumulation and yields are predicted to decline in Guayas but they are predicted to increase in Los Ríos. The distinct biomass and yield responses for the two regions mainly derive from temperature and precipitation anomalies in the warmer lowlands of Guayas that have a negative impact on rice productivity in the region.

Crop duration was also predicted to change with duration increasing in the Los Ríos region, but decreasing in the Guayas region.

Our analysis, the first assessment of the impact of climate change on rice yields in Ecuador, indicates the importance of fine-scale analyses using simple models to make predictions that are relevant to regional production scenarios. The utility of using climate

data to make predictions about crop yields should incentivize the further setting up of good-quality agro-meteorological stations based on cropland covers for Ecuador.

Supplementary Materials: The following supporting information can be downloaded at: https://www.mdpi.com/article/10.3390/agriculture12111828/s1, Table S1: HadGEM-RegCM4 dynamical downscaling model configuration (a). Kobayashi's very simple model (VSM) configuration input (b); Table S2: Downscaled climatological data (base period 1975–2005) for the Guayas (a) and Los Ríos (b) Provinces , extracted based on LULC rice crop areas. Reference [83] are cited in the supplementary materials.

Author Contributions: Conceptualization, D.P., S.F., A.D. and S.V.C.; methodology, D.P., S.V.C. and A.D.; software, D.P., S.F. and S.V.C.; validation, D.P., A.D., M.T.-U., E.A., V.P. and S.F.; formal analysis, D.P., A.D. and V.P.; investigation, D.P., V.P., M.T.-U. and E.A.; resources, S.F. and A.D.; data curation, D.P., V.P. and S.F.; writing, D.P.; original draft preparation, D.P., A.D., S.F. and F.G.H.; writing—review and editing, D.P., F.G.H., E.A. and M.T.-U.; visualization, D.P. and S.F.; supervision, S.F., A.D. and S.V.C.; project administration, S.F. All authors have read and agreed to the published version of the manuscript.

Funding: This research received no external funding.

Institutional Review Board Statement: Not applicable.

Informed Consent Statement: Not applicable.

Data Availability Statement: Not applicable.

Acknowledgments: The authors recognize the National Council for Scientific and Technological Development (CNPq, Brazil) and the Coordination for the Improvement of Higher Education Personnel (CAPES, Brazil). Diego Portalanza also recognizes the Organization of American States (OAS) and the Coimbra Group of Brazilian Universities (GCUB), with the support of the Division of Educational Topics of the Ministry of Foreign Affairs of Brazil (MRE) on behalf of the OAS Partnerships Program for Education and Training (PAEC OAS-GCUB) for the doctoral academic scholarship.

Conflicts of Interest: The authors declare no conflict of interest.

Abbreviations

The following abbreviations are used in this manuscript:

HadGEM2-ES	Hadley Centre Global Environment Model version 2;
DSSAT	Decision Support System for Agrotechnology Transfer;
CORDEX	Coordinated Regional Climate 269 Downscaling Experiment;
RegCM4	Regional Climate Modeling 141 System;
GDAL	Geospatial Data Abstraction Software Library;
NetCDF	Network Common Data Form;
IPCC	Intergovernmental Panel on Climate Change;
LULC	Land use and land cover;
SWAT	Soil and Water Assessment Tool;
RMSEn	Normalized root mean square error;
RMSE	Root mean square error;
VSM	Very simple model;
NCL	Research Command Language;
RCP	Representative concentration pathways;
GOF	Goodness-of-fit measures;
CO2	Carbon dioxide;
MAE	Mean absolute error;
GCM	Global climate models;
RCM	Regional climate model;
LAI	Leaf area index;
RP	Reference period;
FP	Future period;
RH	Relative humidity.

References

1. Kong, W.; Zhong, H.; Gong, Z.; Fang, X.; Sun, T.; Deng, X.; Li, Y. Meta-analysis of salt stress transcriptome responses in different rice genotypes at the seedling stage. *Plants* **2019**, *8*, 64. [CrossRef] [PubMed]
2. Yuan, S.; Peng, S.; Li, T. Evaluation and application of the ORYZA rice model under different crop managements with high-yielding rice cultivars in central China. *Field Crops Res.* **2017**, *212*, 115–125. [CrossRef]
3. Seck, P.A.; Diagne, A.; Mohanty, S.; Wopereis, M. Crops that feed the world 7: Rice. *Food Secur.* **2012**, *4*, 7–24. [CrossRef]
4. Godfray, H.C.J.; Beddington, J.R.; Crute, I.R.; Haddad, L.; Lawrence, D.; Muir, J.F.; Pretty, J.; Robinson, S.; Thomas, S.M.; Toulmin, C. Food Security: The Challenge of Feeding 9 Billion People. *Science* **2010**, *327*, 812–818. [CrossRef]
5. Ullah, A.; Nawaz, A.; Farooq, M.; Siddique, K.H. Agricultural innovation and sustainable development: A case study of rice–wheat cropping systems in South Asia. *Sustainability* **2021**, *13*, 1965. [CrossRef]
6. Sivakumar, M.V.; Gommes, R.; Baier, W. Agrometeorology and sustainable agriculture. *Agric. For. Meteorol.* **2000**, *103, 11–26*. [CrossRef]
7. ESPAC. *Encuesta de Superficie y Producción Agropecuaria Continua ESPAC 2017 Contenidos*; INEC: Quito, Ecuador, 2017.
8. Horgan, F.G.; Zhu, Q.; Portalanza, D.E.; Felix, M.I. Costs to Ecuador's rice sector during the first decade of an apple snail invasion and policy recommendations for regions at risk. *Crop Prot.* **2021**, *148*, 105746. [CrossRef]
9. INEC. Censo Nacional Agropecuario. 2019. Available online: https://www.ecuadorencifras.gob.ec/censo-nacional-agropecuario/ (accessed on 20 May 2021).
10. FAO. Crops. 2017. License: CC BY-NC-SA 3.0 IGO. Available online: https://www.fao.org/faostat/en/#home (accessed on 20 May 2021).
11. Alava, M.F.; Poaquiza, J.T.; Castillo, G.H. La producción arrocera del Ecuador. *Rev. Espac.* **2018**, *39*, 1–16.
12. Marcelo, C. *Rendimiento de Arroz en Cáscara, Primer Cuatrimestre 2017*; Dirección de Análisis y Procesamiento de la Información Coordinación General del Sistema de Información Nacional Ministerio de Agricultura, Ganadería: Quito, Ecuador, 2017.
13. Herrera-Fontana, M.E.; Chisaguano, A.M.; Villagomez, V.; Pozo, L.; Villar, M.; Castro, N.; Beltran, P. Food insecurity and malnutrition in vulnerable households with children under 5 years on the Ecuadorian coast: A post-earthquake analysis. *Rural Remote Health* **2020**, *20*, 5237. [CrossRef]
14. Trisasongko, B.H.; Panuju, D.R.; Harimurti; Ramly, A.F.; Subroto, H. Rapid assessment of agriculture vulnerability to drought using GIS. *Int. J. Technol.* **2016**, *7*, 114–122. [CrossRef]
15. Wang, J.; Wang, E.; Yang, X.; Zhang, F.; Yin, H. Increased yield potential of wheat-maize cropping system in the North China Plain by climate change adaptation. *Clim. Chang.* **2012**, *113*, 825–840. [CrossRef]
16. Aryal, J.P.; Sapkota, T.B.; Khurana, R.; Khatri-Chhetri, A.; Rahut, D.B.; Jat, M.L. Climate change and agriculture in South Asia: Adaptation options in smallholder production systems. *Environ. Dev. Sustain.* **2020**, *22*, 5045–5075. [CrossRef]
17. Huong, N.T.L.; Bo, Y.S.; Fahad, S. Economic impact of climate change on agriculture using Ricardian approach: A case of northwest Vietnam. *J. Saudi Soc. Agric. Sci.* **2019**, *18*, 449–457. [CrossRef]
18. Yohannes, H. A Review on Relationship between Climate Change and Agriculture. *J. Earth Sci. Clim. Chang.* **2015**, *7*, 1–8. [CrossRef]
19. IPCC. IPCC Fifth Assessment Synthesis Report-Climate Change 2014 Synthesis Report. In *IPCC Fifth Assessment Synthesis Report-Climate Change 2014*; Synthesis Report; IPCC: Geneva, Switzerland, 2014.
20. IPCC. Summary for Policymakers. In *Climate Change 2013—The Physical Science Basis*; IPCC, Ed.; Cambridge University Press: Cambridge, UK, 2013; pp. 1–30. [CrossRef]
21. Gupta, R.; Mishra, A. Climate change induced impact and uncertainty of rice yield of agro-ecological zones of India. *Agric. Syst.* **2019**, *173*, 1–11. [CrossRef]
22. Muis, S.; Apecechea, M.I.; Dullaart, J.; de Lima Rego, J.; Madsen, K.S.; Su, J.; Yan, K.; Verlaan, M. A High-Resolution Global Dataset of Extreme Sea Levels, Tides, and Storm Surges, Including Future Projections. *Front. Mar. Sci.* **2020**, *7*, 263. [CrossRef]
23. Sun, Q.; Miao, C.; Duan, Q.; Ashouri, H.; Sorooshian, S.; Hsu, K. A Review of Global Precipitation Data Sets: Data Sources, Estimation, and Intercomparisons. *Rev. Geophys.* **2018**, *56*, 79–107. [CrossRef]
24. van Vuuren, D.P.; Edmonds, J.; Kainuma, M.; Riahi, K.; Thomson, A.; Hibbard, K.; Hurtt, G.C.; Kram, T.; Krey, V.; Lamarque, J.F.; et al. The representative concentration pathways: An overview. *Clim. Chang.* **2011**, *109*, 5–31. [CrossRef]
25. Manzanas, R.; Gutiérrez, J.M.; Fernández, J.; van Meijgaard, E.; Calmanti, S.; Magariño, M.E.; Cofiño, A.S.; Herrera, S. Dynamical and statistical downscaling of seasonal temperature forecasts in Europe: Added value for user applications. *Clim. Serv.* **2018**, *9*, 44–56. [CrossRef]
26. Maraun, D. Bias Correcting Climate Change Simulations—A Critical Review. *Curr. Clim. Chang. Rep.* **2016**, *2*, 211–220. [CrossRef]
27. Amiri, E.; Razavipour, T.; Farid, A.; Bannayan, M. Effects of crop density and irrigation management on water productivity of rice production in northern Iran: Field and modeling approach. *Commun. Soil Sci. Plant Anal.* **2011**, *42*, 2085–2099. [CrossRef]
28. Ebrahimirad, H.; Amiri, E.; Babazadeh, H.; Sedghi, H. Calibration and evaluation of ceres-rice model under different density and water managements. *Appl. Ecol. Environ. Res.* **2018**, *16*, 6469–6482. [CrossRef]
29. Kobayashi, K. A very simple model of crop growth: Derivation and application. *Int. Rice Res. Notes* **1994**, 50–51. ISSN: 0115-0944
30. Pirmoradian, N.; Sepaskhah, A. A Very Simple Model for Yield Prediction of Rice under Different Water and Nitrogen Applications. *Biosyst. Eng.* **2006**, *93*, 25–34. [CrossRef]

31. Rebolledo, M.; Ramírez-Villegas, J.; Graterol, E.; Hernández-Varela, C.; Rodríguez-Espinoza, J.; Petro-Páez, E.; Pinzón, S.; Heinemann, A.; Rodríguez-Baide, J.; van den Berg, M. *Modelación del Arroz en Latinoamérica: Estado del Arte y Base de Datos para Parametrización*; Technical Report; Publications Office of the European Union: Luxembourg, 2018. [CrossRef]
32. MAE-MAGAP. *Protocolo Metodológico para la Elaboración del Mapa de Cobertura y Uso de la Tierra del Ecuador Continental 2013–2014. Escala 1:100.000*; Technical Report; Ministerio del Ambiente del Ecuador y Ministerio de Agricultura, Ganadería, Acuacultura y Pesca: Quito, Ecuador, 2015.
33. GDAL/OGR Contributors. GDAL/OGR Geospatial Data Abstraction software Library. *Open Source Geospat. Found.* **2022**. [CrossRef]
34. Bellouin, N.; Collins, W.J.; Culverwell, I.D.; Halloran, P.R.; Hardiman, S.C.; Hinton, T.J.; Jones, C.D.; McDonald, R.E.; McLaren, A.J.; O'Connor, F.M.; et al. The HadGEM2 family of Met Office Unified Model climate configurations. *Geosci. Model Dev.* **2011**, *4*, 723–757. [CrossRef]
35. Collins, W.; Bellouin, N.; Doutriaux-Boucher, M.; Gedney, N.; Hinton, T.; Jones, C.D.; Liddicoat, S.; Martin, G.; O'Connor, F.; Rae, J.; et al. *Evaluation of HadGEM2 Model*; Technical Note 74; Meteorological Office Hadley Centre: Exeter, UK, 2008.
36. Dickinson, R.; Errico, R.; Giorgi, F.; Bates, G. A regional climate model for the western United States. *Clim. Chang.* **1989**, *15*, 383–422. [CrossRef]
37. Giorgi, F.; Coppola, E.; Solmon, F.; Mariotti, L.; Sylla, M.; Bi, X.; Elguindi, N.; Diro, G.; Nair, V.; Giuliani, G.; et al. RegCM4: Model description and preliminary tests over multiple CORDEX domains. *Clim. Res.* **2012**, *52*, 7–29. [CrossRef]
38. Schulzweida, U. CDO User' s Guide. Climate Data Operators Version 1.5.9. *MAX-PLANCK-INSTITUT FÜR METEOROLOGIE*. Hamburg, Germany. 2012. Available online: http://www.idris.fr/media/ada/cdo.pdf (accessed on 20 May 2021).
39. Meier-fleischer, K.; Böttinger, M.; Haley, M.; Meier-fleischer, K. NCL User Guide. *German Climate Computing Center (Deutsches Klimarechenzentrum, DKRZ)*. Hamburg, Germany. 2019. Available online: https://www.ncl.ucar.edu/Document/Manuals/NCL_User_Guide/ (accessed on 20 May 2021).
40. Bjørnæs, C. *A Guide to Representative Concentration Pathways*; Center for International Climate and Environmental Research: Oslo, Norway, 2015. Available online: https://cicero.oslo.no/en (accessed on 25 May 2021).
41. IPCC. *Climate Change 2013—The Physical Science Basis*; Cambridge University Press: Cambridge, UK, 2014. [CrossRef]
42. Riahi, K.; Rao, S.; Krey, V.; Cho, C.; Chirkov, V.; Fischer, G.; Kindermann, G.; Nakicenovic, N.; Rafaj, P. RCP 8.5—A scenario of comparatively high greenhouse gas emissions. *Clim. Chang.* **2011**, *109*, 33–57. [CrossRef]
43. Emanuel, K.A.; Živković-Rothman, M. Development and Evaluation of a Convection Scheme for Use in Climate Models. *J. Atmos. Sci.* **1999**, *11*, 1766–1782. [CrossRef]
44. Holtslag, A.A.M.; De Bruijn, E.I.F.; Pan, H.L. A High Resolution Air Mass Transformation Model for Short-Range Weather Forecasting. *Mon. Weather Rev.* **1990**, *118*, 1561–1575. [CrossRef]
45. Pal, J.S.; Small, E.E.; Eltahir, E.A. Simulation of regional-scale water and energy budgets: Representation of subgrid cloud and precipitation processes within RegCM. *J. Geophys. Res. Atmos.* **2000**, *105*, 29579–29594. [CrossRef]
46. Shaman, J.; Pitzer, V.E.; Viboud, C.C.; Lipsitch, M.; Grenfell, B.T.; Lipsitch, M. Absolute humidity and the seasonal onset of influenza in the continental US. *PLoS Biol.* **2010**, *8*, e1000316. [CrossRef]
47. Li, H.; Sheffield, J.; Wood, E.F. Bias correction of monthly precipitation and temperature fields from Intergovernmental Panel on Climate Change AR4 models using equidistant quantile matching. *J. Geophys. Res.* **2010**, *115*, D10101. [CrossRef]
48. Sachindra, D.A.; Huang, F.; Barton, A.; Perera, B.J.C. Statistical downscaling of general circulation model outputs to precipitation—Part 2: Bias-correction and future projections. *Int. J. Climatol.* **2014**, *34*, 3282–3303. [CrossRef]
49. Turco, M.; Llasat, M.C.; Herrera, S.; Gutiérrez, J.M. Bias correction and downscaling of future RCM precipitation projections using a MOS-analog technique. *J. Geophys. Res.* **2017**, *122*, 2631–2648. [CrossRef]
50. COPERNICUS CLIMATE CHANGE SERVICE (C3S). ERA5: Fifth generation of ECMWF atmospheric reanalyses of the global climate. *Copernic. Clim. Chang. Serv. Clim. Data Store (CDS)* **2017**, *15*, 2020.
51. Cucchi, M.; Weedon, G.; Amici, A.; Bellouin, N.; Lange, S.; Schmied, H.M.; Hersbach, H.; Buontempo, C. WFDE5: Bias adjusted ERA5 reanalysis data for impact studies. *Earth Syst. Sci. Data Discuss.* **2020**, *12*, 2097–2120. [CrossRef]
52. Hersbach, H.; Bell, B.; Berrisford, P.; Horányi, A.; Sabater, J.M.; Nicolas, J.; Radu, R.; Schepers, D.; Simmons, A.; Soci, C.; et al. Global reanalysis: Goodbye ERA-Interim, hello ERA5. *ECMWF Newsl.* **2019**, *159*, 17–24. [CrossRef]
53. Chai, T.; Draxler, R.R. Root mean square error (RMSE) or mean absolute error (MAE)?—Arguments against avoiding RMSE in the literature. *Geosci. Model Dev.* **2014**, *7*, 1247–1250. [CrossRef]
54. Willmott, C.J. On the validation of models. *Phys. Geogr.* **1981**, *2*, 184–194. [CrossRef]
55. Zambrano, M.B. Package 'hydroGOF': Goodness-of-Fit Functions for Comparison of Simulated and Observed Hydrological Time Series. *Swat*. R Package Version 0.4-0. 2017. Available online: https://helpx.adobe.com/acrobat/using/allow-or-block-links-internet.html (accessed on 20 May 2021). [CrossRef]
56. RStudio. *RStudio: Integrated Development Environment for R*; RStudio, PBC: Boston, MA, USA, 2017. Available online: http://www.rstudio.com/ (accessed on 20 May 2021).
57. Wickham, H. *ggplot2*; Springer: New York, NY, USA, 2009. [CrossRef]
58. Wickham, H. *Package 'ggplot2' Title Create Elegant Data Visualisations Using the Grammar of Graphics*; Technical Report; Springer: New York, NY, USA, 2020.

59. Gaydon, D.; Balwinder-Singh; Wang, E.; Poulton, P.; Ahmad, B.; Ahmed, F.; Akhter, S.; Ali, I.; Amarasingha, R.; Chaki, A.; et al. Evaluation of the APSIM model in cropping systems of Asia. *Field Crop. Res.* **2017**, *204*, 52–75. [CrossRef]
60. Mysiak, J.; Surminski, S.; Thieken, A.; Mechler, R.; Aerts, J. Brief communication: Sendai framework for disaster risk reduction – success or warning sign for Paris? *Nat. Hazards Earth Syst. Sci.* **2016**, *16*, 2189–2193. [CrossRef]
61. Lizarralde, G.; Bornstein, L.; Robertson, M.; Gould, K.; Herazo, B.; Petter, A.M.; Páez, H.; Díaz, J.H.; Olivera, A.; González, G.; et al. Does climate change cause disasters? How citizens, academics, and leaders explain climate-related risk and disasters in Latin America and the Caribbean. *Int. J. Disaster Risk Reduct.* **2021**, *58*, 102173. [CrossRef]
62. Scheid, A.; Hafner, J.; Hoffmann, H.; Kächele, H.; Sieber, S.; Rybak, C. Fuelwood scarcity and its adaptation measures: An assessment of coping strategies applied by small-scale farmers in Dodoma region, Tanzania. *Environ. Res. Lett.* **2018**, *13*, 095004. [CrossRef]
63. Dinh, K.D.; Anh, T.N.; Nguyen, N.Y.; Bui, D.D.; Srinivasan, R. Evaluation of grid-based rainfall products and water balances over the Mekong river Basin. *Remote Sens.* **2020**, *12*, 1858. [CrossRef]
64. Gutowski, W.J., Jr.; Giorgi, F.; Timbal, B.; Frigon, A.; Jacob, D.; Kang, H.S.; Krishnan, R.; Lee, B.; Lennard, C.; Nikulin, G.; et al. WCRP COordinated Regional Downscaling EXperiment (CORDEX): A diagnostic MIP for CMIP6. *Geosci. Model Dev. Discuss.* **2016**, *9*, 4087–4095. [CrossRef]
65. Chun, J.A.; Li, S.; Wang, Q.; Lee, W.S.; Lee, E.J.; Horstmann, N.; Park, H.; Veasna, T.; Vanndy, L.; Pros, K.; et al. Assessing rice productivity and adaptation strategies for Southeast Asia under climate change through multi-scale crop modeling. *Agric. Syst.* **2016**, *143*, 14–21. [CrossRef]
66. Su, P.; Zhang, A.; Wang, R.; Wang, J.; Gao, Y.; Liu, F. Prediction of future natural suitable areas for rice under representative concentration pathways (RCPs). *Sustainability* **2021**, *13*, 1580. [CrossRef]
67. Li, T.; Angeles, O.; Marcaida, M.; Manalo, E.; Manalili, M.P.; Radanielson, A.; Mohanty, S. From ORYZA2000 to ORYZA (v3): An improved simulation model for rice in drought and nitrogen-deficient environments. *Agric. For. Meteorol.* **2017**, *237*, 246–256. [CrossRef]
68. Arunrat, N.; Pumijumnong, N.; Hatano, R. Predicting local-scale impact of climate change on rice yield and soil organic carbon sequestration: A case study in Roi Et Province, Northeast Thailand. *Agric. Syst.* **2018**, *164*, 58–70. [CrossRef]
69. Erda, L.; Wei, X.; Hui, J.; Yinlong, X.; Yue, L.; Liping, B.; Liyong, X. Climate change impacts on crop yield and quality with CO_2 fertilization in China. *Philos. Trans. R. Soc. B Biol. Sci.* **2005**, *360*, 2149–2154. [CrossRef] [PubMed]
70. Mandal, U.; Sena, D.R.; Dhar, A.; Panda, S.N.; Adhikary, P.P.; Mishra, P.K. Assessment of climate change and its impact on hydrological regimes and biomass yield of a tropical river basin. *Ecol. Indic.* **2021**, *126*, 107646. [CrossRef]
71. Araya, A.; Kisekka, I.; Lin, X.; Vara Prasad, P.; Gowda, P.; Rice, C.; Andales, A. Evaluating the impact of future climate change on irrigated maize production in Kansas. *Clim. Risk Manag.* **2017**, *17*, 139–154. [CrossRef]
72. Lv, C.; Huang, Y.; Sun, W.; Yu, L.; Zhu, J. Response of rice yield and yield components to elevated [CO_2]: A synthesis of updated data from FACE experiments. *Eur. J. Agron.* **2020**, *112*, 125961. [CrossRef]
73. Hu, S.; Wang, Y.; Yang, L. Response of rice yield traits to elevated atmospheric CO_2 concentration and its interaction with cultivar, nitrogen application rate and temperature: A meta-analysis of 20 years FACE studies. *Sci. Total. Environ.* **2021**, *764*, 142797. [CrossRef]
74. Bergamaschi, H.; Bergonci, J. *As Plantas e o Clima: Princípios e Aplicações*; Agrolivros: Guaíba, Brazil, 2017; 351p.
75. Coast, O.; Ellis, R.H.; Murdoch, A.J.; Quiñones, C.; Jagadish, K.S.V. High night temperature induces contrasting responses for spikelet fertility, spikelet tissue temperature, flowering characteristics and grain quality in rice. *Funct. Plant Biol.* **2015**, *42*, 149. [CrossRef]
76. Ding, Y.; Wang, W.; Song, R.; Shao, Q.; Jiao, X.; Xing, W. Modeling spatial and temporal variability of the impact of climate change on rice irrigation water requirements in the middle and lower reaches of the Yangtze River, China. *Agric. Water Manag.* **2017**, *193*, 89–101. [CrossRef]
77. Acharjee, T.K.; van Halsema, G.; Ludwig, F.; Hellegers, P.; Supit, I. Shifting planting date of Boro rice as a climate change adaptation strategy to reduce water use. *Agric. Syst.* **2019**, *168*, 131–143. [CrossRef]
78. Dharmarathna, W.R.S.S.; Herath, S.; Weerakoon, S.B. Changing the planting date as a climate change adaptation strategy for rice production in Kurunegala district, Sri Lanka. *Sustain. Sci.* **2014**, *9*, 103–111. [CrossRef]
79. Asseng, S.; Ewert, F.; Rosenzweig, C.; Jones, J.W.; Hatfield, J.L.; Ruane, A.C.; Boote, K.J.; Thorburn, P.J.; Rötter, R.P.; Cammarano, D.; et al. Uncertainty in simulating wheat yields under climate change. *Nat. Clim. Chang.* **2013**, *3*, 827–832. [CrossRef]
80. Ruane, A.C.; Major, D.C.; Winston, H.Y.; Alam, M.; Hussain, S.G.; Khan, A.S.; Hassan, A.; Al Hossain, B.M.T.; Goldberg, R.; Horton, R.M.; et al. Multi-factor impact analysis of agricultural production in Bangladesh with climate change. *Glob. Environ. Chang.* **2013**, *23*, 338–350. [CrossRef]
81. Horgan, F.G.; Romena, A.M.; Bernal, C.C.; Almazan, M.L.P.; Ramal, A.F. Stem borers revisited: Host resistance, tolerance, and vulnerability determine levels of field damage from a complex of Asian rice stemborers. *Crop. Prot.* **2021**, *142*, 105513. [CrossRef] [PubMed]
82. Horgan, F.G. Potential for an Impact of Global Climate Change on Insect Herbivory in Cereal Crops. In *Crop Protection Under Changing Climate*; Springer International Publishing: Cham, Switzerland, 2020; pp. 101–144. [CrossRef]
83. Holtslag, A.A.M.; Van Meijgaard, E.; De Rooy, W.C. A comparison of boundary layer diffusion schemes in unstable conditions over land. *Bound.-Layer Meteorol.* **1995**, *76*, 69–95. [CrossRef]